

Strategies for advantageous differential transport of ions in magnetic fusion devices

E. J. Kolmes, I. E. Ochs, and N. J. Fisch

Citation: *Physics of Plasmas* **25**, 032508 (2018); doi: 10.1063/1.5023931

View online: <https://doi.org/10.1063/1.5023931>

View Table of Contents: <http://aip.scitation.org/toc/php/25/3>

Published by the *American Institute of Physics*



**COMPLETELY
REDESIGNED!**

**PHYSICS
TODAY**

Physics Today Buyer's Guide
Search with a purpose.

Strategies for advantageous differential transport of ions in magnetic fusion devices

E. J. Kolmes,^{a)} I. E. Ochs, and N. J. Fisch

Department of Astrophysical Sciences, Princeton University, Princeton, New Jersey 08544, USA and
 Princeton Plasma Physics Laboratory, Princeton, New Jersey 08540, USA

(Received 29 January 2018; accepted 9 March 2018; published online 26 March 2018)

In a variety of magnetized plasma geometries, it has long been known that highly charged impurities tend to accumulate in regions of higher density. This “collisional pinch” is modified in the presence of additional forces, such as those might be found in systems with gravity, fast rotation, or non-negligible space charge. In the case of a rotating, cylindrical plasma, there is a regime in which the radially outermost ion species is intermediate in both mass and charge. This could have implications for fusion devices and plasma mass filters. *Published by AIP Publishing.*

<https://doi.org/10.1063/1.5023931>

I. INTRODUCTION

The diffusive transport of plasma across a magnetic field is a subject of longstanding importance throughout plasma physics. From tokamaks^{1,2} and stellarators³ to magnetic mirrors^{4,5} and low-temperature plasmas,^{6–8} problems related to cross-field transport are prominent both for their intrinsic scientific significance and for their practical implications in the design and analysis of plasma-based technology. The transport properties of high- Z_a impurities are of particular interest in fusion plasmas, where heavier elements from the wall can reduce the performance of a fusion device. They are also very important in plasma mass filters, which are designed to sort the material in a plasma based on mass.^{9–17}

Early in the development of plasma transport theory, it was predicted that high- Z_a impurities in a predominantly low- Z_b magnetized background plasma would demonstrate a dramatic pinch effect.^{18–20} In particular, in steady state, the impurity density n_a and the background ion density n_b in an isothermal plasma satisfy

$$\frac{(n_b)^{Z_a/Z_b}}{n_a} = \text{const.} \quad (1)$$

If impurities are introduced in small quantities at the low-density edge of a magnetically confined plasma, Eq. (1) implies that they will be strongly concentrated in the high-density core of the plasma.¹⁹ The same result has been found in neoclassical transport in a wide range of parameter regimes.^{21–23}

There have been experimental indications of a pinch of impurities in plasma devices.^{24–26} However, the impurity pinch may be mitigated in some practical contexts. For instance, although neoclassical corrections can increase the speed of the pinch, analysis and experiments have shown that the effect might be reduced by temperature gradients in some regimes.^{22,26,27} This paper will not deal with the effects

of turbulence, though of course the presence of turbulent transport can change all of these results.^{28,29}

However, Eq. (1) is no longer accurate in the presence of an external potential. Certain corrections associated with centrifugal or electrostatic forces acting on a magnetically confined plasma have been studied already, both experimentally and with analytical and computational models. This work has mostly been in the context of tokamak physics^{27,30–35} and plasma mass filters.^{9–14,36–38} This paper will derive a more general form of Eq. (1) that can account for the presence of an arbitrary external potential. The case of a centrifugal potential is equivalent to an expression used in the context of plasma centrifuges.^{12–14}

This generalized formulation makes it possible to intuitively describe the differential transport of various ion species in a variety of different systems. Beyond being academically interesting, this description serves a practical purpose, revealing regimes in which desirable and undesirable species can be differentially transported with greater freedom. For instance, in p-¹¹B fusion, boron ions and protons fuse to form helium. In a fully ionized system, both boron and helium ash are more massive and highly charged than the protons. However, boron (as a fuel ion) is desirable to concentrate in the core of a fusion device, whereas the accumulation of helium ash would reduce fusion performance. Equation (1) does not offer any way of choosing a proton profile that would draw in boron while pushing out helium. The generalized formula does describe a window in parameter space in which such an outcome should be possible. Thus, understanding the detailed transport behavior of different species in a plasma could be important for increasing fusion efficiency.

This paper is organized as follows: Sec. II contains a brief derivation of Eq. (1), generalized to include external potentials, and shows how the collisional pinch and Gibbs distribution emerge naturally as limits of the resulting impurity distribution. Section III discusses some of the implications of these results in a gravitational potential. Section IV presents a similar analysis for a centrifugal potential and discusses strategies for flushing impurities and fusion products in different scenarios.

^{a)}ekolmes@princeton.edu

II. DERIVATION OF GENERALIZED PINCH

Cross-field collisional transport is driven primarily by interactions between unlike particles.³⁹ Consider a plasma with two ion species, indexed by subscripts a and b , in a magnetic field with no externally imposed forces other than $\mathbf{j} \times \mathbf{B}$ forces. If this system contains pressure gradients, some cross-field motion will occur via diamagnetic drifts. This motion will be perpendicular both to ∇p and to \mathbf{B} . In a cylindrical geometry with an axial magnetic field and $p = p(r)$, it will result in azimuthal flows.

When there are diamagnetic drifts in a collisional magnetized plasma, there is an additional cross-field transport mechanism that arises from the relative diamagnetic motion of the particle species. This relative motion causes a frictional force, which in turn drives an $\mathbf{F} \times \mathbf{B}$ drift parallel to the pressure gradients. Equation (1) can be derived from the condition that the frictional forces between these two species vanish (i.e., that there is no relative velocity). This derivation has been done previously in both the fluid picture⁴⁰ and the single-particle picture.⁴¹ This section will briefly replicate and extend the argument in the fluid picture, allowing for an additional species-dependent external potential Φ_s with a gradient parallel to that of the pressure.

The force felt by a particle of species a as a result of friction with another species b can be modeled as $-m_s \nu_{ab}(\mathbf{v}_a - \mathbf{v}_b)$. The force on species b is the same up to exchange of indices, where the conservation of momentum requires that the collision frequencies satisfy $n_a m_a \nu_{ab} = n_b m_b \nu_{ba}$. Consider a system without temperature gradients or shear strain forces, but with density gradients perpendicular to \mathbf{B} . Assume the different species all have the same temperature. The fluid momentum equation is

$$m_a \frac{d\mathbf{v}_a}{dt} = q_a \mathbf{v}_a \times \mathbf{B} - \frac{T \nabla n_a}{n_a} - \nabla \Phi_a + \sum_s m_a \nu_{as} (\mathbf{v}_s - \mathbf{v}_a). \quad (2)$$

From this, and neglecting the inertial terms, the flux of species a in the direction parallel to the pressure gradients due to collisions with species b is

$$\Gamma_a = -\frac{1}{2} \rho_s^2 n_a \nu_{ab} \left[\frac{\nabla n_a}{n_a} - \frac{Z_a}{Z_b} \frac{\nabla n_b}{n_b} + \frac{\nabla \Phi_a}{T} - \frac{Z_a}{Z_b} \frac{\nabla \Phi_b}{T} \right] \cdot \hat{\mathbf{e}}_n. \quad (3)$$

Here, ρ_s is the Larmor radius for species s and $\hat{\mathbf{e}}_n$ is a unit vector in the direction of ∇n_a . When there is an external potential, the relative motion between the species depends on both diamagnetic and $-\nabla \Phi_s \times \mathbf{B}$ drifts.

When Γ_a vanishes, Eq. (3) is equivalent to the condition that

$$(n_a e^{\Phi_a/T}) \propto (n_b e^{\Phi_b/T})^{Z_a/Z_b}. \quad (4)$$

Equation (4) is the generalization of Eq. (1) in the presence of an external potential. When $\nabla \Phi_a = \nabla \Phi_b = \mathbf{0}$, it reduces to the original pinch. If the profile of species b is completely supported by the potential Φ_b (that is, if n_b

assumes a Gibbs distribution), then the spatial dependence on the right-hand side cancels, so species a must also be Gibbs-distributed. For cases between the Gibbs distribution and the original pinch, Eq. (4) describes a whole family of solutions that fall between the Gibbs distribution and the classic pinch. If only part of the pressure profile of species b is supported by the potential Φ_b , Eq. (4) implies that the pinch acts only on the part of the profiles not supported by Φ_a and Φ_b . That is, if $n_s = \tilde{n}_s e^{-\Phi_s/T}$, then $\tilde{n}_a \propto \tilde{n}_b^{Z_a/Z_b}$. Interestingly, if $\Phi_a/\Phi_b = Z_a/Z_b$, then Eq. (4) reduces to Eq. (1); an electrostatic potential and the collisional pinch both tend to concentrate highly charged particles, but they do so to the same extent and their effects do not stack.

Nothing in this derivation assumed anything in particular about the relative masses, densities, or charges of the species a and b , so long as all species are magnetized. However, the flux of species a due to interactions with species b scales with ν_{ab} . If Eq. (4) is not satisfied for a pair of species a and b , the size of the resulting flux will depend on their collision frequency. In other words, when ν_{ab} is larger, the system will tolerate smaller deviations from Eq. (4) in order to be in steady state on any given timescale.

For comparable target densities, ion-ion collision frequencies are typically much larger than ion-electron collision frequencies. For this reason, it often makes sense to treat Eq. (4) as a requirement for ion density profiles with respect to one another rather than for ion profiles with respect to the electron profile.

It is important to note that Eq. (4) is not, on its own, a prescription for how n_a reacts to the introduction of an external potential. It describes a relationship between n_a and n_b ; finding n_a requires specifying n_b . As the strengths of the potentials Φ_a and Φ_b vary, Eq. (4) predicts very different behavior of the impurity profile depending on how the background ion profile changes.

III. DISTRIBUTION LIMITS IN A SIMPLE LINEAR POTENTIAL

Consider a multiple-species plasma with some species-dependent potential Φ_s and a constant magnetic field $\mathbf{B} = B\hat{\mathbf{z}}$. If every species satisfies Eq. (4) with respect to a fixed reference species, then they automatically satisfy Eq. (4) with respect to one another. Suppose some reference ion species has mass m_b and charge $Z_b e$. Then, define a “steepness parameter” α_b for which

$$n_b \propto \exp \left[-\frac{\alpha_b \Phi_b}{T} \right]. \quad (5)$$

In fact, α_b could be a function rather than a constant, and the results in this section would continue to hold. The steepness parameter α_b measures how steep the reference distribution is relative to its thermodynamic equilibrium distribution.

Equation (4) can be rewritten in terms of a set of steepness parameters as

$$n_a \propto \exp \left[-\frac{\alpha_a \Phi_b}{T} \right], \quad (6)$$

$$\alpha_a = \frac{Z_a}{Z_b} (\alpha_b - 1) + \frac{\Phi_a}{\Phi_b}. \quad (7)$$

Because electrostatic potentials cancel from Eq. (4), it is often convenient (and equally valid) not to include electrostatic terms in the Φ_s potentials used in Eqs. (5)–(7).

Consider, for example, a plasma in a linear gravitational potential $\Phi_a = m_a g x$. For this choice of potential, Eq. (4) becomes

$$n_a = (\text{const}) n_b^{Z_a/Z_b} \exp \left[Z_a \left(\frac{m_b}{Z_b} - \frac{m_a}{Z_a} \right) \frac{g x}{T} \right] \quad (8)$$

and Eq. (7) becomes

$$\alpha_a = \frac{Z_a}{Z_b} (\alpha_b - 1) + \frac{m_a}{m_b}. \quad (9)$$

It is immediately apparent that both the charge ratio Z_a/Z_b and mass ratio m_a/m_b now play a role in determining the impurity distribution. Define the thermodynamic scale height λ_b by

$$\lambda_b \doteq \frac{T}{m_b g}. \quad (10)$$

For the gravitational potential, any constant α_s has an intuitive interpretation: it is the inverse scale height of the distribution, normalized by λ_b .

Take α_b as a free parameter that is imposed; in effect, it represents how far a reference profile is from thermodynamic equilibrium, with $\alpha_b = 1$ corresponding to thermodynamic equilibrium (or rather, to what would be thermodynamic equilibrium if species b encounters no electric fields). A specific choice of α_b then imposes a different α_a on each other plasma species via Eq. (9).

Equation (9) shows that the balance between the charge-dependent and mass-dependent parts of α_a depends critically on the magnitude of α_b . In the potential-free limit $\alpha_b \rightarrow \infty$, Eq. (9) becomes

$$\alpha_a = \frac{Z_b}{Z_a} \alpha_b, \quad (11)$$

which is simply a reformulation of the collisional pinch Eq. (1). If instead $\alpha_b = 1$, i.e., the reference species has reached a Gibbs distribution with respect to the gravitational potential, then

$$\alpha_a = \frac{m_a}{m_b} \quad (12)$$

so that

$$n_a(x) = n_{a0} e^{-x m_a / m_b \lambda_b} = n_{a0} e^{-x / \lambda_a}, \quad (13)$$

where $\lambda_a = T/m_a g$ is the thermodynamic scale height for species a in the gravitational field. In other words, if the background approaches a Gibbs distribution with respect to the

gravitational field, any impurities naturally approach such a state as well.

IV. CENTRIFUGING ION SPECIES

In a rotating system with several ion species, the balance between charge-dependent and mass-dependent effects can lead to useful outcomes. Consider an isothermal cylindrical system undergoing solid-body rotation, so that there is an effective centrifugal potential $\Phi_a(r) = -m_a \Omega^2 r^2 / 2$. In terms of an arbitrary reference species b , Eq. (4) becomes

$$n_a = (\text{const}) n_b^{Z_a/Z_b} \exp \left[Z_a \left(\frac{m_a}{Z_a} - \frac{m_b}{Z_b} \right) \frac{\Omega^2 r^2}{2T} \right]. \quad (14)$$

That is

$$\begin{aligned} & \left(n_a \exp \left[-\frac{m_a \Omega^2 r^2}{2T} \right] \right)^{1/Z_a} \\ &= (\text{const}) \left(n_b \exp \left[-\frac{m_b \Omega^2 r^2}{2T} \right] \right)^{1/Z_b}. \end{aligned} \quad (15)$$

This is equivalent to a previously derived result.^{12,13} Given a fixed n_b , whether the distribution n_a will be steeper or less steep than it would have been without rotation depends on the relative charge-to-mass ratios of species a and b , as was true in the gravitational case.

For a centrifugal potential, Eq. (5) is

$$n_b \propto \exp \left[\frac{\alpha_b m_b \Omega^2 r^2}{2T} \right]. \quad (16)$$

Due to centrifugal forces, this would mean that for $\alpha_b = 1$ the reference ions are distributed according to a centrifugal Gibbs distribution, namely, flung towards high radius, with minimum density at $r = 0$. If the reference ions are so distributed, then by Eq. (15), it is immediately evident that so are all ions. For $\alpha_b > 1$, the reference ions are more concentrated yet at large radius, which means that, relatively speaking, all ions are more concentrated at large radii compared to their centrifugal Gibbs distributions. For $\alpha_b < 1$, ions are less steeply distributed. However, if $\alpha_b < 0$, the ions are inverted with respect to their centrifugal Gibbs distributions; in this case, the distribution is peaked at the center rather than at the periphery. This is the case of general interest in fusion devices, where fusion occurs preferentially in a central hot and dense core of plasma.

Note that not all the α_a need have the same sign, or if they do have the same sign, their relative ordering can be a function of α_b . It is of interest to arrange for fuel ions to be concentrated preferentially in the interior near $r = 0$, while fusion byproducts or other contaminants are comparatively less concentrated in the interior. For the centrifugal potential, $\Phi_a/\Phi_b = m_a/m_b$, so Eq. (9) is the governing equation for the steepness parameters.

Since the reference species b is arbitrary, it can be taken to be protons (whether or not protons are actually present is immaterial; α_H can still be treated as a free parameter of the system). With that choice, Eq. (9) becomes

$$\alpha_a = Z_a(\alpha_H - 1) + \frac{m_a}{m_p}. \quad (17)$$

As was the case with the gravitational potential, there are two limits: one in which the charge-dependent term dominates and the result approaches Eq. (1), and another in which the mass-dependent term dominates and the result approaches a Gibbs distribution with respect to the centrifugal potential. As before, because the steepness parameters are defined with respect to the centrifugal potential alone (and not the electric potential), $\alpha_r = 1$ is only the true thermodynamic equilibrium if there are no electric fields.

When $\alpha_b < 1$, it can happen that the species that is radially the furthest out has neither the highest Z_a nor the highest m_a . For instance, consider a fully ionized plasma of protons, boron-11, helium-4, and tungsten-184. This might model a p-¹¹B fusion plasma with thermalized fusion products and some tungsten impurities. In a non-rotating system, the outermost species would always be the p or the ¹⁸⁴W, since these have the smallest and largest charges, respectively. In a rotating plasma with a centrifugal Gibbs distribution, the outermost species would always be the ¹⁸⁴W, because of its large mass. But away from these two limits, it is possible to find cases in which any of these species are the furthest out, including the ⁴He. This result could not be achieved using just the physics of the conventional pinch or the physics of a conventional centrifuge. Essentially, it is possible when the classical pinch and the centrifugal force pull in opposite directions.

Figure 1 shows the relative steepness of the hydrogen, helium, and boron for a variety of choices of α_H . In fusion devices, it is typically advantageous to limit the buildup of fusion products and impurities like tungsten relative to the fuel ions. There is a region in Fig. 1 in which the fuel ions and thermalized ⁴He particles are all peaked toward small r but where the ⁴He is less concentrated in the core than the fuel ions. This happens when

$$-2 < \alpha_H < -\frac{4}{3}. \quad (18)$$

There is something special about the case of α ash in a p-¹¹B plasma: the fusion product has a charge that is between the charges of the two fuel ions. Consider a rotating system with ion species i, j , and k , in which $Z_i < Z_j < Z_k$. Then there exists a choice of α_i for which $\alpha_j > \alpha_i, \alpha_k$ if and only if

$$\frac{m_k - m_j}{Z_k - Z_j} < \frac{m_j - m_i}{Z_j - Z_i}. \quad (19)$$

For any reference species b , the width of this region will be

$$\Delta\alpha_b = \frac{Z_b}{m_b} \left[\frac{m_j - m_i}{Z_j - Z_i} - \frac{m_k - m_j}{Z_k - Z_j} \right]. \quad (20)$$

Very similar analyses can be done for a variety of choices of fuel and impurity ions. For instance, for a p-¹¹B plasma, there is also a somewhat smaller region (not marked in the figure) in which the fusion products and tungsten impurities are both further out than the fuel ions. This happens when

$$-\frac{110}{73} < \alpha_H < -\frac{4}{3}. \quad (21)$$

The large Z of the impurities makes the transition between inwardly and outwardly peaked ¹⁸⁴W quite abrupt. Of course, this is all for fully ionized tungsten; partially ionized tungsten would have a larger window (which would be a superset of the original window) due to its lower charge state.

In a bulk deuterium-tritium plasma, thermalized α particles will be radially further out than the fuel ions if any of the following (equivalent) conditions are met:

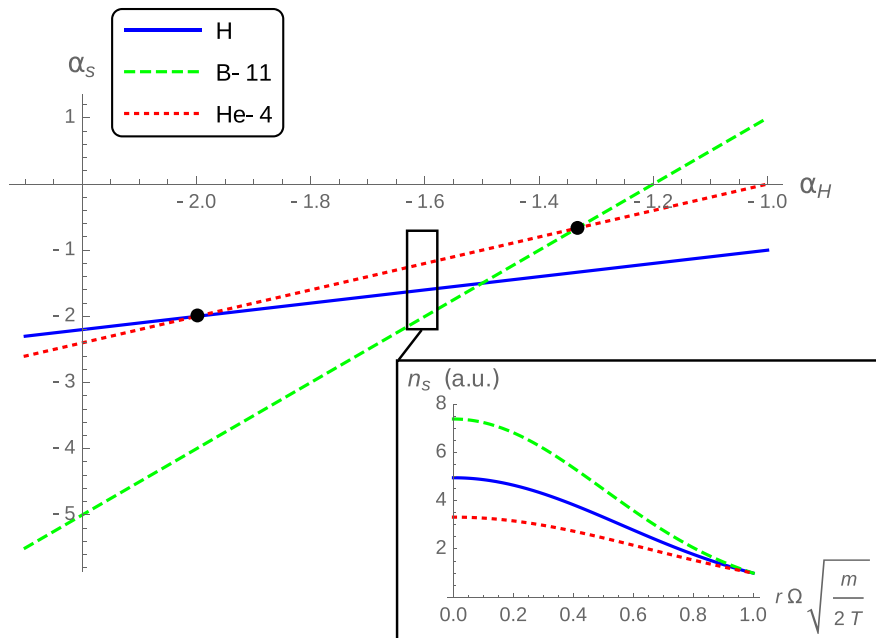


FIG. 1. The steepness parameters α_s of three particle species as a function of the hydrogen steepness parameter α_H in a centrifugal potential. A more negative α_s corresponds to a profile that is more peaked at small r . The region in which the alpha particles are less concentrated in the core than the proton and ¹¹B populations (despite the fact that the alpha particles are intermediate in charge and mass) is $-2 < \alpha_H < -4/3$. This region is marked by dots. The inset figure shows spatial profiles corresponding to a choice of $\alpha_H = -1.6$, which falls in this region; it can be seen that the ¹¹B is twice as peaked relative to its edge density as the ⁴He.

$$\alpha_D > 1, \quad (22)$$

$$\alpha_T > 2, \quad (23)$$

$$\alpha_{\text{He}} > 2. \quad (24)$$

Rather than a window, the requirement is a simple inequality. The favorable ion distributions happen when both fuel and fusion product profiles are peaked at the radial edges of the device, though they do not have to be as peaked as they would be in a centrifugal Gibbs distribution.

In a rotating plasma composed mostly of deuterium and ^3He , the condition for thermalized α particles to be the furthest out can be written in any of the following ways:

$$\alpha_D > 0, \quad (25)$$

$$\alpha_{^3\text{He}} > -1, \quad (26)$$

$$\alpha_{\text{He}} > 0. \quad (27)$$

This is qualitatively similar to the condition for a D-T plasma. However, D- ^3He reactions also produce protons, and there is no choice of steepness parameters for which thermalized protons will be radially further out than deuterium.

The conversion between a choice of α_b and a density profile $n_a(r)$ requires information about the temperature and rotation rate of the plasma. Define a thermal Mach number $\text{Ma}_{\text{th}} \doteq r\Omega/\sqrt{2T/m_b}$ for the reference species. For solid-body rotation, Ma_{th} will be linear in r . In terms of this parameter

$$n_b \propto \exp[\alpha_b \text{Ma}_{\text{th}}^2]. \quad (28)$$

The regimes identified in this section are constraints on α_b . The size of Ma_{th} will rescale the density profile that corresponds to a given choice of α_b , so that the same α_b will result in a steeper density profile in a system with a larger Ma_{th} . For a constraint like Eq. (21), this means that a smaller Ma_{th} pushes the favorable regime toward flatter profiles and, in some sense, makes the space of favorable profiles smaller.

For most realistic scenarios, these regions in α_b space do not require very steep profiles. If a plasma has much less energy in its rotational motion than in its thermal motion, and if the steepness parameters are $\sim \pm 1$, Eq. (16) implies that n will not be very steep for any of the species. For instance, for a 1 keV cylindrical plasma with $\Omega = 100$ kHz, the proton profile corresponding to $\alpha_H = -3/2$ (where the protons are the reference species) would be

$$n_p \approx n_{p0} e^{-(r/3.6\text{ m})^2}. \quad (29)$$

In other words, even a very high rotation rate would not require unrealistically steep profiles in order to fall in the regimes described by, e.g., Eqs. (18) and (21). In some cases, the challenge for practical devices would more likely be to increase Ma_{th} so that the favorable density profiles are less flat.

Of course, this kind of calculation could also be useful for plasma mass filter applications. For instance, in order to drive a heavy impurity with $m_a > m_b$ and $Z_a > Z_b$ radially outwards, it is better to have a background profile that is flat than one that is peaked at the core, since this prevents the

pinch effect from competing with the centrifugal effects. This kind of question has been studied experimentally;⁴² the work by Skibenko *et al.* included consideration of the role of $n_a(\mathbf{r})$ in these problems, though not the role of Φ_a .

It is important to note that the analysis in this section has not included the effects of temperature gradients or net particle fluxes. Either of these could be important for the behavior of a real device. Nonetheless, the simple calculation presented here raises some interesting practical possibilities.

V. DISCUSSION

In the presence of an external potential, the collisional impurity pinch contains two parts. One part depends on the impurities' charge and on how close the background ions are to thermodynamic equilibrium. The other part depends only on the external potential acting on the impurities. It is possible to affect the balance between these terms by changing the external potential or by changing the background ion density profile. The ability to predict and control the behavior of the pinch could be of use in any application where impurity concentrations matter.

These results relate the different density profiles to one another, but they do not fully specify the different profiles. To do that would require two things. First, there would have to be a way of specifying the normalization of each profile; this might be done with a boundary condition or with a condition on the total number of particles. Second, one profile (or linear combination of profiles) must be determined independently. Control over this profile is a practical problem which is not addressed here. It might be done with neutral particle sources, like pellet injection, or through waves, as in alpha channeling.⁴³ Both of these processes will be balanced by ambipolar particle diffusion out of the device. This paper also does not address the problem of how to set up a potential Φ_a . A centrifugal potential, for instance, might be set up by generating perpendicular \mathbf{E} and \mathbf{B} fields, though the self-consistent behavior of such systems can be complex.^{44–47} Rotation profiles can also be manipulated with compressional techniques.^{48,49} Note that an \mathbf{E} field used to induce $\mathbf{E} \times \mathbf{B}$ rotation would have no direct effect on the relationship between the density profiles beyond its role in setting up a centrifugal potential. This is due to the cancellation of electrostatic potentials from Eq. (4), as was discussed in Sec. II.

Of course, the calculations presented here do not present a comprehensive picture of all ways to modify the impurity pinch and their implications. This paper does not discuss the implications of impurities that are hotter or colder than the background plasma, nor does it deal with spatial temperature gradients. Temperature gradients are known to affect the impurity pinch in different ways, depending on the details of the system.^{22,23,40,50} This is an area of active research; for instance, there has been recent progress in the possibility of using temperature gradients to mitigate the impurity pinch in stellarators.^{51,52}

These calculations are also far from being a comprehensive treatment of the effects of rotation and of electrostatic potentials in a practical device. For instance, the tendency of rotational effects to cause uneven distributions across flux

surfaces in a toroidal geometry can be important in some systems.^{31,34} This paper has not included the effects of viscosity; this is safe for systems sufficiently close to solid-body rotation, but not for more general rotation profiles.

This study was motivated in part by a larger investigation of the Wave-Driven Rotating Torus (WDRT) plasma confinement concept. In a WDRT, minor-radial electric fields and toroidal magnetic fields provide the rotational transform by setting up $\mathbf{E} \times \mathbf{B}$ rotation.^{53,54} The transport of minority ions in such a device is complicated but important, since one way of maintaining the large voltage gradients would be to preferentially remove helium ash from the device (by α channeling or otherwise). The results discussed here suggest that electric fields themselves will not affect the impurity accumulation in a WDRT, and that the rotation induced by the crossed fields will change the impurity transport in a way that might be advantageous.

ACKNOWLEDGMENTS

We would like to acknowledge S. Davidovits, V. I. Geyko, A. S. Glasser, R. Gueroult, M. Mlodik, and J.-M. Rax for helpful conversations. This work was supported by DOE Grant Nos. DE-SC0016072, DE-FG02-97ER25308, and DE-AC02-09CH1-1466.

- ¹S. P. Hirshman and D. J. Sigmar, *Nucl. Fusion* **21**, 1079 (1981).
- ²M. H. Redi, S. A. Cohen, and E. J. Synakowski, *Nucl. Fusion* **31**, 1689 (1991).
- ³S. Braun and P. Helander, *Phys. Plasmas* **17**, 072514 (2010).
- ⁴R. F. Post, *Nucl. Fusion* **27**, 1579 (1987).
- ⁵R. Gueroult and N. J. Fisch, *Phys. Plasmas* **19**, 112105 (2012).
- ⁶A. Smirnov, Y. Raitses, and N. J. Fisch, *Phys. Plasmas* **11**, 4922 (2004).
- ⁷C. L. Ellison, Y. Raitses, and N. J. Fisch, *Phys. Plasmas* **19**, 013503 (2012).
- ⁸D. Curreli and F. F. Chen, *Plasma Sources Sci. Technol.* **23**, 064001 (2014).
- ⁹B. Bonnevier, *Ark. Fys.* **33**, 255 (1966).
- ¹⁰B. Lehnert, *Nucl. Fusion* **11**, 485 (1971).
- ¹¹T. Hellsten, *Nucl. Instrum. Methods* **145**, 425 (1977).
- ¹²M. Krishnan, *Phys. Fluids* **26**, 2676 (1983).
- ¹³M. Geva, M. Krishnan, and J. L. Hirshfield, *J. Appl. Phys.* **56**, 1398 (1984).
- ¹⁴D. A. Dolgolenko and Yu. A. Muromkin, *Phys.-Usp.* **60**, 994 (2017).
- ¹⁵I. E. Ochs, R. Gueroult, N. J. Fisch, and S. J. Zweben, *Phys. Plasmas* **24**, 043503 (2017).
- ¹⁶V. B. Yuferov, S. V. Katrechko, V. O. Ilichova, S. V. Shariy, A. S. Svichkar, M. O. Shvets, E. V. Mufel, and A. G. Bobrov, *Prob. At. Sci. Tech.* **113**, 118 (2018).
- ¹⁷R. Gueroult, J.-M. Rax, S. J. Zweben, and N. J. Fisch, *Plasma Phys. Controlled Fusion* **60**, 014018 (2018).
- ¹⁸L. Spitzer, *Astrophys. J.* **116**, 299 (1952).
- ¹⁹J. B. Taylor, *Phys. Fluids* **4**, 1142 (1961).
- ²⁰S. I. Braginskii, "Transport processes in a plasma," in *Reviews of Plasma Physics*, edited by M. A. Leontovich (Consultants Bureau, New York, 1965), Vol. 1, p. 205.
- ²¹J. W. Connor, *Plasma Phys.* **15**, 765 (1973).
- ²²P. H. Rutherford, *Phys. Fluids* **17**, 1782 (1974).
- ²³F. L. Hinton and T. B. Moore, *Nucl. Fusion* **14**, 639 (1974).
- ²⁴S. A. Cohen, J. L. Cecchi, and E. S. Marmor, *Phys. Rev. Lett.* **35**, 1507 (1975).
- ²⁵G. Fussman, A. R. Field, A. Kallenbach, K. Krieger, K.-H. Steuer, and the ASDEX Team, *Plasma Phys. Controlled Fusion* **33**, 1677 (1991).
- ²⁶R. Dux, C. Giroud, K.-D. Zastrow, and JET EFDA Contributors, *Nucl. Fusion* **44**, 260 (2004).
- ²⁷M. R. Wade, W. A. Houlberg, and L. R. Baylor, *Phys. Rev. Lett.* **84**, 282 (2000).
- ²⁸K. Ida, M. Yoshinuma, M. Osakabe, K. Nagaoka, M. Yokoyama, H. Funaba, C. Suzuki, T. Ido, A. Shimizu, I. Murakami, N. Tamura, H. Kasahara, Y. Takeiri, K. Ikeda, K. Tsumori, O. Kaneko, S. Morita, M. Goto, K. Tanaka, K. Narihara, T. Minami, I. Yamada, and LHD Experimental Group, *Phys. Plasmas* **16**, 056111 (2009).
- ²⁹A. Loarte, M. L. Reinke, A. R. Polevoi, M. Hosokawa, M. Chilenski, N. Howard, A. Hubbard, J. W. Hughes, J. E. Rice, J. Walk, Alcator C-Mod Team, F. Köchl, T. Pütterich, R. Dux, and V. E. Zhogolev, *Phys. Plasmas* **22**, 056117 (2015).
- ³⁰K. H. Burrell, T. Ohkawa, and S. K. Wong, *Phys. Rev. Lett.* **47**, 511 (1981).
- ³¹M. Romanelli and M. Ottaviani, *Plasma Phys. Controlled Fusion* **40**, 1767 (1998).
- ³²R. J. Taylor, T. A. Carter, J.-L. Gauvreau, P.-A. Gourdain, A. Grossman, D. J. LaFontaine, D. C. Pace, L. W. Schmitz, A. E. White, and T. F. Yates, *Nucl. Fusion* **45**, 1634 (2005).
- ³³P.-A. Gourdain, *Phys. Plasmas* **13**, 072502 (2006).
- ³⁴C. Angioni and P. Helander, *Plasma Phys. Controlled Fusion* **56**, 124001 (2014).
- ³⁵F. J. Casson, C. Angioni, E. A. Belli, R. Bilato, P. Mantica, T. Odstreil, T. Pütterich, M. Valisa, L. Garzotti, C. Giroud, J. Hobirk, C. F. Maggi, J. Mlynar, M. L. Reinke, JET EFDA Contributors, and ASDEX-Upgrade Team, *Plasma Phys. Controlled Fusion* **57**, 014031 (2015).
- ³⁶A. J. Fetterman and N. J. Fisch, *Phys. Plasmas* **18**, 094503 (2011).
- ³⁷R. Gueroult, J.-M. Rax, and N. J. Fisch, *Phys. Plasmas* **21**, 020701 (2014).
- ³⁸J.-M. Rax and R. Gueroult, *J. Plasma Phys.* **82**, 595820504 (2016).
- ³⁹C. L. Longmire and M. N. Rosenbluth, *Phys. Rev.* **103**, 507 (1956).
- ⁴⁰P. Helander and D. J. Sigmar, *Collisional Transport in Magnetized Plasmas* (Cambridge University Press, Cambridge, UK, 2002).
- ⁴¹I. E. Ochs, J.-M. Rax, R. Gueroult, and N. J. Fisch, *Phys. Plasmas* **24**, 083503 (2017).
- ⁴²E. I. Skibenko, Y. V. Kovtun, A. I. Skibenko, I. N. Onischenko, and V. B. Yuferov, *Tech. Phys.* **54**, 1380 (2009).
- ⁴³N. J. Fisch and J.-M. Rax, *Phys. Rev. Lett.* **69**, 612 (1992).
- ⁴⁴T. M. O'Neil, *Phys. Fluids* **24**, 1447 (1981).
- ⁴⁵J. Ghosh, R. C. Elton, H. R. Griem, A. Case, R. Ellis, A. B. Hassam, S. Messer, and C. Teodorescu, *Phys. Plasmas* **11**, 3813 (2004).
- ⁴⁶R. F. Ellis, A. Case, R. Elton, J. Ghosh, H. Griem, A. Hassam, R. Lunsford, S. Messer, and C. Teodorescu, *Phys. Plasmas* **12**, 055704 (2005).
- ⁴⁷M. Amoretti, C. Canali, C. Carraro, V. Lagomarsino, A. Odino, G. Testera, and S. Zavatarelli, *Phys. Plasmas* **13**, 012308 (2006).
- ⁴⁸V. I. Geyko and N. J. Fisch, *Phys. Rev. Lett.* **110**, 150604 (2013).
- ⁴⁹V. I. Geyko and N. J. Fisch, *Phys. Plasmas* **24**, 022113 (2017).
- ⁵⁰F. L. Hinton and R. D. Hazeltine, *Rev. Mod. Phys.* **48**, 239 (1976).
- ⁵¹P. Helander, S. L. Newton, A. Mollén, and H. M. Smith, *Phys. Rev. Lett.* **118**, 155002 (2017).
- ⁵²S. L. Newton, P. Helander, A. Mollén, and H. M. Smith, *J. Plasma Phys.* **83**, 905830505 (2017).
- ⁵³J.-M. Rax, R. Gueroult, and N. J. Fisch, *Phys. Plasmas* **24**, 032504 (2017).
- ⁵⁴I. E. Ochs and N. J. Fisch, *Phys. Plasmas* **24**, 092513 (2017).